Ceramics International 44 (2018) 8505–8513

Contents lists available at ScienceDirect

Ceramics International

journal homepage: www.elsevier.com/locate/ceramint

Evaluation of oxidation behaviors of HfC-SiC ultra-high temperature ceramics at above 2500 °C via oxyacetylene torch

Young-Hoon Seong[a,b,1], Changyeon Baek[a,1], Joo-Hyung Kim[a], Jung Hoon Kong[a], Dong Seok Kim[a,c], Sea-Hoon Lee[d], Do Kyung Kim[a,*]

[a] Department of Materials Science and Engineering, Korea Advanced Institute of Science and Technology (KAIST), Yuseong-gu, Daejeon 34141, Republic of Korea
[b] Korea Institute of Energy Research (KIER), Yuseong-gu, Daejeon 34129, Republic of Korea
[c] Korea Atomic Energy Research Institute (KAERI), Yuseong-Gu, Daejeon 34057, Republic of Korea
[d] Korea Institute of Materials Science (KIMS), Changwon, Gyeongnam 51508, Republic of Korea

ARTICLE INFO

Keywords:
HfC-SiC
UHTCs
Oxidation behavior
Oxyacetylene torch

ABSTRACT

Development of materials highly resistant to harsh conditions (including ultra-high temperature) has been a crucial issue for the development of next-generation hyper velocity vehicles. HfC-SiC ceramics have been attractive as suitable candidates for these applications owing to their extraordinarily high melting temperatures. Here, HfC-SiC ceramics with ultra-fine grains, prepared via reactive spark plasma sintering, were tested under an oxyacetylene torch flame for relatively long exposure times (5–30 min). The oxidation behaviors of the samples were carefully characterized by microstructural analysis. Although porous structures were formed due to the generation and escape of gas phases, the mixture of oxidized species composed of HfO_2 granules and melted SiO_2 phase, acted as an excellent barrier under the condition of severe high-temperature oxidation.

1. Introduction

Increasing interest in re-entry hypersonic vehicles and weapons has driven demand for materials that might be used for leading-edge, nose-tip, and propulsion-system components. The buffer materials for these applications are exposed to extreme environments including aerodynamic heating introduced by continuous friction at the interface between the material and the atmosphere. To protect the main body of projectiles, these protecting materials must withstand the severe thermal shock and oxidation that occur at ultra-high temperatures (> 2000 °C) [1,2]

Among many kinds of protecting materials that survive these severe conditions, Hf-based ceramics such as HfB_2 and HfC are among the most promising candidates. HfC ceramics are also known as materials that are durable at very high temperature, along with other carbide ceramics including TaC and ZrC [3]. In addition, the oxide scales (e.g., HfO_2 or HfO_{2-x}) that form as a result of the oxidation of HfC ceramics, have a very high melting temperature, over 2500 °C [3,4]. This high melting temperature of these oxidized scales enables the underlying materials to survive even in ambient (oxidizing) atmosphere. Despite the merits of HfC ceramics, they are also known to have both a low sinterability due to their high melting temperature and gas evolution problem when it is oxidized [5–8]. Therefore, it is important that many researchers have found that addition of SiC to form HfC-SiC ceramics maximizes their thermal resistance by enhancing their sinterability [9,10]. The added SiC can also support oxidation resistance by forming SiO_2 scale at lower temperature under oxidizing conditions [11,12]. For these reasons, the HfC-SiC ceramics have been investigated as various forms of composite structure, such as the inter-layered structure of HfC-SiC with BN or graphite, the multilayer coating for C-C composites, and infiltrated HfC into a C-C matrix; to avoid fracture due to the low thermal shock resistance of HfC-SiC ceramics [13–16].

It is also very important to determine the durability of such materials before making actual vehicles because a great deal of time and expense will be needed to make the final hypersonic vehicles. Therefore, evaluation of these materials must precede actual applications. High-temperature testing using an oxyacetylene torch is one of the most frequently used methods, and has the merits of simplicity, low cost, and sufficiently high temperature (~ 3000 °C) with respect to the oxygen to acetylene gas ratio [13–32]. There have been a few reports from studies to investigate the high-temperature oxidation behavior of other UHTCs under the severe exposure to oxyacetylene flame for up to 40 min [18] Here, we discuss the oxidation behaviors of nano-grained HfC-SiC ceramics under this harsh condition using a newly designed

* Corresponding author.
E-mail address: dkkim@kaist.ac.kr (D.K. Kim).
[1] Equal contributors.

https://doi.org/10.1016/j.ceramint.2018.02.049
Received 9 August 2017; Received in revised form 2 February 2018; Accepted 5 February 2018
Available online 06 February 2018
0272-8842/

oxyacetylene torch testing system. The time-dependent change in the oxidation scale and ablation rate, and the corresponding microstructural aspects were carefully provided to explain the oxidation behavior of fine-grained HfC-SiC ceramics prepared via reactive spark plasma sintering.

2. Experimental section

2.1. Preparation of HfC-SiC composite ceramics

HfC nanopowder (particle size: 100 – 200 nm), $HfSi_2$ (particle size: 1–2 μm; Alfa Aesar, MA, USA) and carbon black powders (surface area: 50–80 m^2/g, purity: 99.5%; Alfa Aesar, MA, USA) were used as starting materials to prepare dense ceramics. The HfC nanopowder and the $HfSi_2$ – C mixture were mixed with the weight ratio of 6:4 by high-energy ball-milling for 2 h in dry condition using a shaker mill (Spex D8000, Spex CertiPrep, Metuchen, NJ) with tungsten carbide balls and jars to yield the well homogenized HfC-34 vol% SiC ceramics. The jars were sealed in a glove box under N_2 gas to suppress oxygen contamination. The mixtures were granulated using a 150 mesh; then loaded into a graphite mold in the glove box. The mixed powders were sintered using reactive spark plasma sintering (SPS) (Dr. Sinter 2020, Sumitomo Coal Mining Co., Tokyo, Japan) at 1900 °C with a uniaxial pressure of 40 MPa for 10 min in vacuum (~20 Pa). HfC-SiC ($\Phi 18 \times 6\ mm^2$) ceramics were obtained by in situ reaction between $HfSi_2$ and carbon during the sintering process.

2.2. Oxyacetylene torch testing and characterization

To investigate the oxidation resistance of the prepared sample, the oxyacetylene torch set-up, which included a temperature monitoring system, a sample holder, mass flow controllers, and a sample stage was custom-built (Fig. 1a). Most of the test procedures (except torch ignition and distance adjustment) were controlled via computer to maintain reproducible test conditions. As-prepared HfC-SiC composite ceramics were polished before the high-temperature oxidation test to minimize the effect from a rough surface. The samples were joined to graphite holders and placed perpendicular to the oxyacetylene torch tip. The distance between the torch tip and the sample surface was 40 mm in all cases to minimize the heat deterioration of the nozzle tip during the tests. After adjusting the distance, the sample stage was retracted to avoid premature heating by the torch flame. When the desired torch flame was ready (O_2 to C_2H_2 gas ratio of 1.3: O_2 = 0.216 l/s; C_2H_2 = 0.167 l/s), the sample stage was advanced to the test position at a speed of 30 mm/s. After the test, we put the torch flame out and kept the tested sample at the test position to let it cool naturally. The heat flux delivered to the surface of the samples was measured using a heat flux gauge (TG1000, Vatell Corp., Christiansburg, VA). The gauge was introduced into the flame, a maximum voltage could be read, and the measurement is repeated three times. The heat flux of the steady oxyacetylene torch was about 800 W/cm^2. This value is similar to the heat flux of the oxyacetylene torch flame reported in the literatures [24,25]. The test conditions included the distance between the samples and the nozzle, the gas flux, and the fuel to oxygen ratio. Fig. 1b includes photographs taken during the oxidation test. The surface temperature of the sample was monitored using a 2-color pyrometer (Pyrospot DSR 10NV, DIAS Infrared GmbH, Dresden, Germany) and recorded in real time in the computer. The spectral range of the pyrometer is 0.7 – 1.1 μm. The inset of Fig. 1b shows the in situ monitoring images obtained by the 2-color pyrometer during the test. The visual changes that occurred during oxyacetylene torch testing could be observed using this in situ monitoring system. To observe the oxidation behavior, samples were prepared and tested for 5, 10, 20, and 30 min.

After the high-temperature oxidation test, the samples were mounted in resin and sectioned at the center of the spot exposed to the torch flame. The cross-sections of the polished samples were

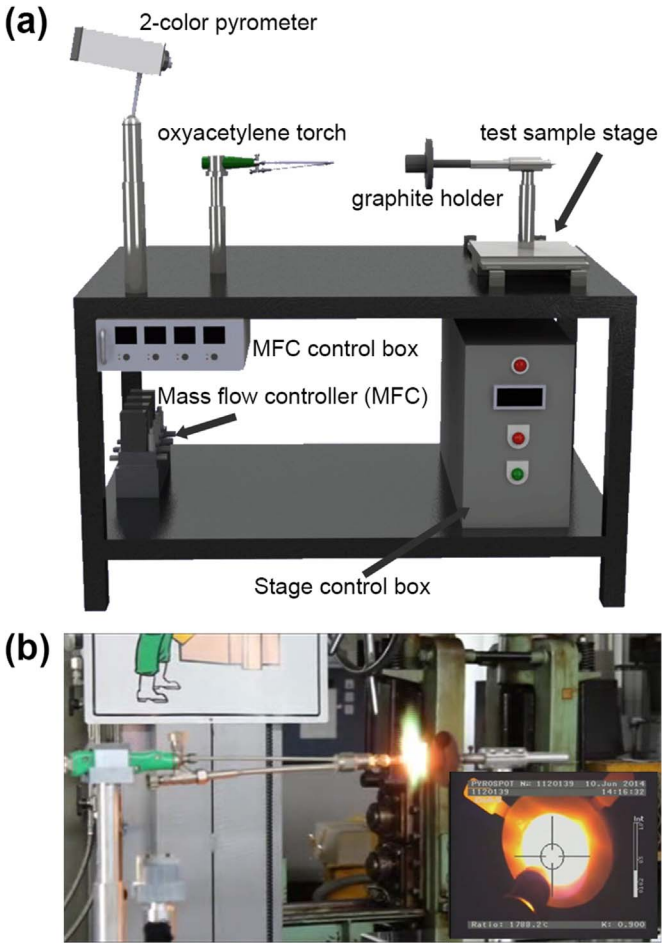

Fig. 1. (a) Scheme for the newly designed oxyacetylene torch set-up, (b) Photographs taken during the actual oxidation test and in situ monitoring images (inset) captured from the recorded video files via a 2-color pyrometer system.

characterized using an optical microscope (OM; Dino-Lite Pro AM-413ZT, AnMo Electronics Corp., Taiwan) and a field-emission scanning electron microscope (FESEM; Model XL30, Philips, The Netherlands) to measure the thicknesses of the residual matrix layer and the surface oxidation layer, respectively.

The crystal structure of the oxidized surfaces was analyzed by X-ray diffractometer (XRD; Rigaku D/Max-RB (12 kW), Tokyo, Japan) with CuKα radiation (λ = 1.5148 Å) operating at 40 kV and 200 mA, with step size of 0.01° at 2° min^{-1} in a 2θ range from 20° to 70°.

3. Results and discussion

The crystal structures of the as-sintered and as-tested samples presented in Fig. 2 clearly show the surface oxidation of the HfC-SiC ceramics. The as-sintered sample mainly had a hafnium carbide phase with a small amount of silicon carbide phase. Successful in situ reaction of carbon with the added $HfSi_2$ occurred during SPS sintering without leaving unreacted species. The surface crystal structures of the oxidation-test samples had HfO_2 phase resulting from the oxidation reaction of HfC. There were no other distinguishable phases such as a crystallized forms of SiO_2 or $HfSiO_4$ (hafnon phase) which could be caused by the solid solution of HfO_2 and SiO_2 [16].

The sample surface was oxidized under the oxyacetylene flame and a clearly defined spot remained on the sample surface exposed to the intense flame. Fig. 3 shows the as-prepared sample and the as-tested samples. The as-prepared sample has the relative density of 100% with average grain size of 0.48 μm for HfC and 0.39 μm for SiC grains respectively. The sample also shows excellent mechanical properties

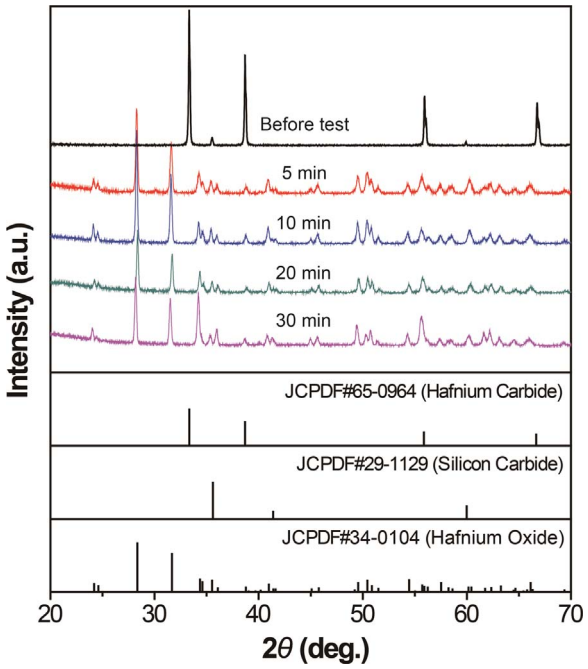

Fig. 2. Crystal structures of the as-sintered HfC-SiC sample and the surface oxide layers formed on the tested sample under the flame of an oxyacetylene torch.

owing to its well-densified microstructure with nano-size grains. The detail information about the prepared HfC-SiC ceramics can be found in the previous study made by L. Feng et al. [10] The as-tested samples were fractured into several pieces by thermal shock during rapid cooling after the test. Fig. 4 shows the surface temperature profile of the prepared HfC-SiC ceramic exposed to the oxyacetylene torch flame for 30 min. The sample heated up immediately after the sample was exposed to the flame. The surface temperature reached ~2500 °C in a few minutes, and gradually increased to 2800 °C as a function of time. The ratio of radiance received by the 2-color pyrometer is independent of target size and of the position of the target within pyrometer field of view. It means that even if the central area of the specimen shone evenly, there might be a temperature gradient. If some of the spots reached a temperature of 2800 °C in the field of view of a 2-color pyrometer, they would have been measured at 2800 °C even if there were areas that did not reach 2800 °C. We believe that the calibration of the 2-color pyrometer is reliable because reasonable results were obtained when testing other ultra-high temperature specimens such as tungsten-rhenium alloy [33]. After the sample was exposed to severe temperature change, the cracks and faint crater traces were observed in the

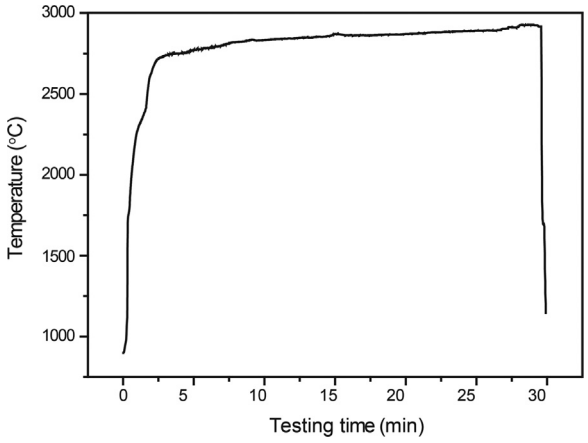

Fig. 4. The recorded surface temperature profile of the HfC-SiC sample during oxidation test (heating) for 30 min.

surface layer with color change from dark grey to white.

Fig. 5a shows the SEM images of the tested samples with different testing time varying from 5 to 30 min. Surface-oxidized layers formed after the test. The thickness of the uneven and crusted layers increased with testing time. Crater-like morphology appeared in the oxidized layers of the samples tested for 20 and 30 min. The dark regions within the oxidized surface layers are voids, and some of the voids were filled with resin during the specimen mounting process. It is thought that the porous oxidized layers originated from severe gas evolution that occurred under the test conditions. The evolved gas phases were accumulated and exhausted through the oxide scale leaving voids during cooling. The void areas were excluded when the thickness of the oxidized layers was measured. Loss of the oxidized species could have occurred during long exposure to the flame, considering previous studies in which the oxidation behaviors of UHTCs were investigated using an oxyacetylene torch. The change in the thickness of the residual matrix also had to be analyzed to confirm whether it went along with the trend of change in the oxidation thickness. To measure the residual matrix thickness, several SEM images were taken for a sample and used together to confirm the thickness of residual thickness. This is because the normal SEM has a small field of view. To minimize the inconvenience and to promote the accuracy of measurement, an optical microscope was used because it has a larger field of view than that of the SEM. Fig. 5b shows the images captured using the optical microscope. From these images, the oxide scale can be more easily observed owing to their definite color difference. Likewise, the residual matrix appears distinct, and this helps to measure the thickness of the matrix phase. The persistence rate (or recession rate) was calculated from the

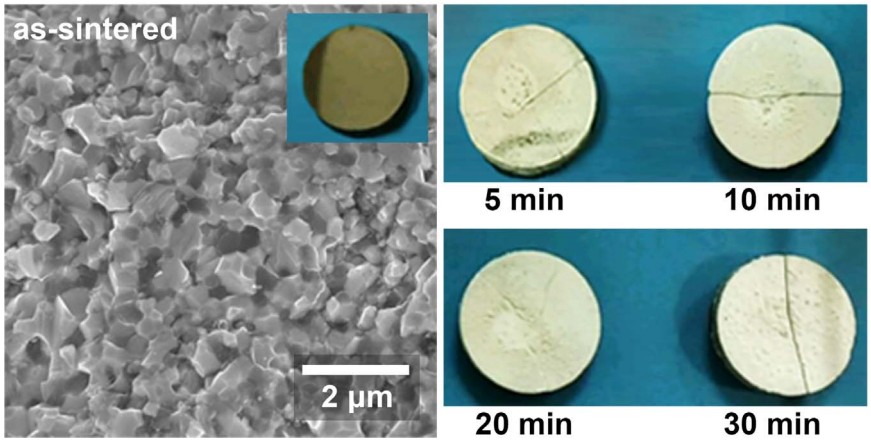

Fig. 3. SEM image of the as-prepared HfC-SiC ceramic and the photographs of as-tested samples exposed to oxyacetylene torch flame for different exposure times.

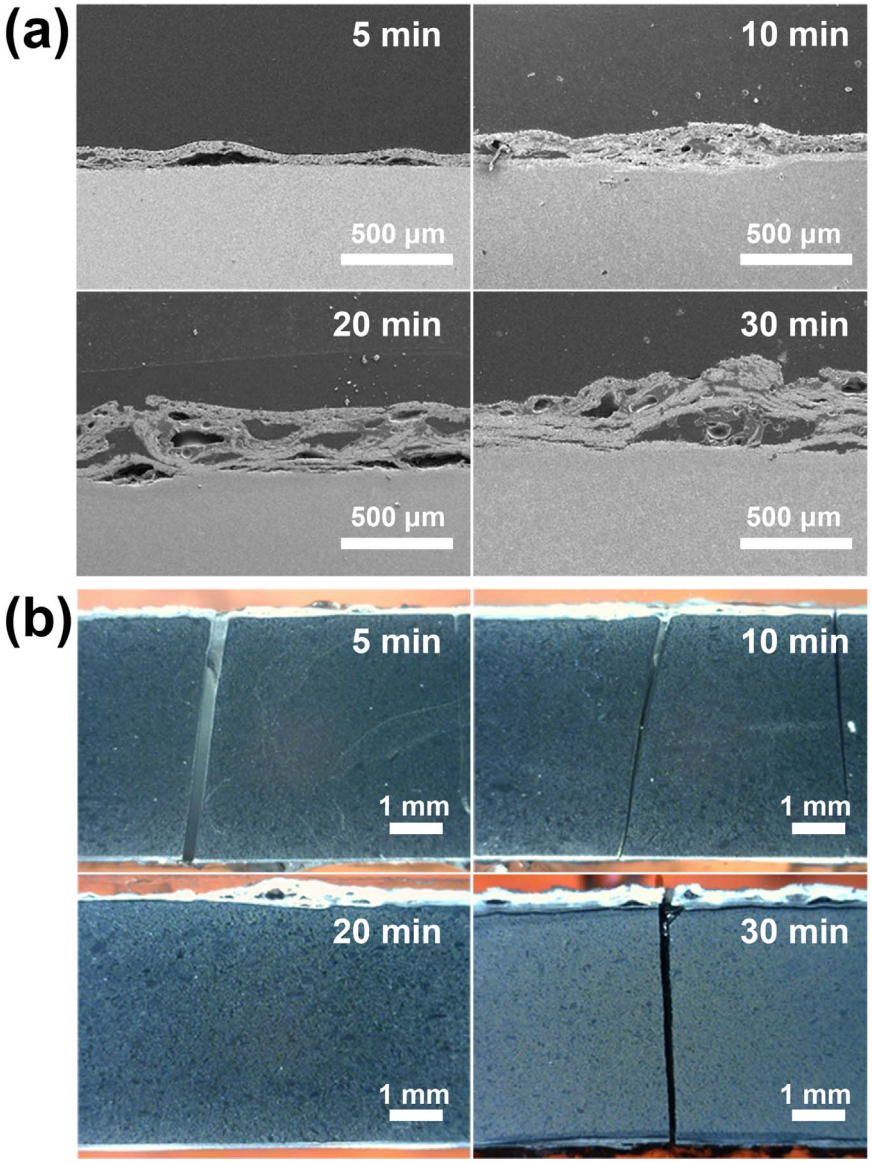

Fig. 5. The cross-sectional SEM images (a) and OM images (b) of the test samples exposed for different times.

difference between the original thicknesses of the samples (t_0) and the residual thickness (t_1) after the test, using the simple equation $(t_0 - t_1)/t_0 * 100$.

The information obtained about the oxidation behavior of the HfC-SiC samples is summarized in Fig. 6. The variation of the oxidation thickness with the heating time (Fig. 6a) shows a parabolic trend. This reduction in the oxidation rate can also be confirmed from the change in residual thickness shown in the inset of Fig. 6b. The thickness of the observed oxidation layer and the recession rate after 30 min exposure, were comparable to the values reported from oxidation tests of different kinds of UHTCs under oxyacetylene torches as shown in Table 1 [13,18,28,31]. This suggests that the oxidation of HfC-SiC under the oxyacetylene torch flame follows reaction diffusion-controlled kinetics [18]. In the low magnification SEM images (Fig. 5a), the surface layer seems porous. From the higher magnification SEM images (Figs. 7 and 8), however, it can be noticed that the surface layer of tested samples is partially densely composed of HfO_2 granules and SiO_2 liquid phase acted as a protective barrier to prevent oxygen diffusion into the HfC-SiC matrix. The parabolic trend in the oxidation behavior generally occurred when the diffusion of oxygen was slowed down due to the presence of the dense surface oxidized layer. The linear ablation rate (Fig. 6b) calculated by dividing the thickness of the residual surface oxidation layers by the heating time could be reduced owing to the presence of this protective surface layer.

Surface and cross-sectional SEM images were used to analyze the oxidation behavior of the HfC-SiC ceramics. Fig. 7 shows the surface morphology of the sample tested for 20 min. Among all the tested samples, the oxidation layer of the sample tested for 20 min was chosen because the oxidation rate declined at this time, and because the sample had features that appeared during both immediate and late periods of the test. There was a common characteristic that the surfaces of the oxidized crusts were porous in all the samples tested. Overall, the samples had rough surface morphology with two distinguishable phases. The main phase (dark) was smooth and wavy without any noticeable boundaries. The other phase (bright) had pebble-like granules a few microns wide. The EDS elemental analysis revealed that the dark area (spot 1) was composed of Si and O, which means that SiO_2 phase was formed the during oxidation test. The SiO_2 liquid phase was consolidated in amorphous phase due to the rapid cooling (quenching) after the test. This could be the reason that the crystallized SiO_2 phases were not identified in the XRD patterns. On the other hand, the bright granules (spot 2) consisted of Hf and O, which implies that these

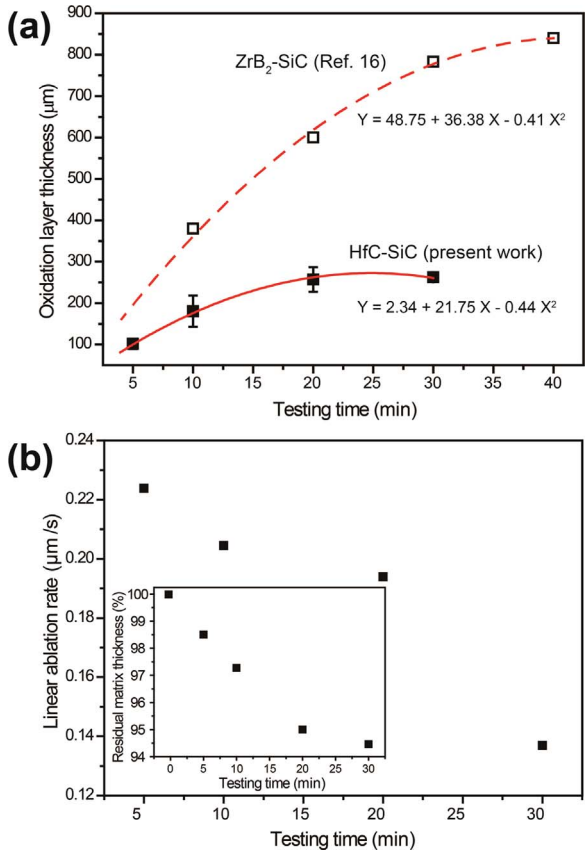

Fig. 6. (a) The surface oxidized layer thickness as a function of testing time measured from the cross-sectional SEM images (b) The calculated linear ablation rate obtained by dividing the thickness of the surface oxidation layers by the test time, and the inset shows the thickness of the residual matrix.

granules are HfO_2 phase. The size of the HfO_2 granules was larger than the average grain size of the as-sintered HfC-SiC sample (~400 nm). The instantaneous oxidation of the HfC grains caused the formation of HfO_2 granules, and the HfO_2 granules grew while floating around in the melted SiO_2 matrix under high temperature. It is also possible that the gaseous phases that occurred during the oxidation test flowed through during this liquid phase. The evacuation of the generated gaseous phases from underneath the surface oxidation layer during the oxidation test, and the influx of oxygen from the surface to the matrix passed through the liquid phase and the bubble-like craters can be seen as evidence of this [15]. Oxygen diffuses through the HfO_2 grain boundary, liquid SiO_2, or the path (pore, crack) created by the degradation of the sample during the ablation test. The SiC of the matrix reacts with diffused oxygen and is oxidized to SiO_2, then melted at high temperature, and viscous flow to the surface by capillary force and volume expansion [11,12]. SiO_2 which was moved to the surface is exposed to high temperature and gas velocity, and is vaporized or blew away from the surface of sample. This process repeated during the test.

As a result of observing the cross-sectional microstructure of the surface layer (Fig. 8(a), region 1), it was found that liquid SiO_2 was distributed directly below the surface in most regions. The solid phase HfO_2 in the form of spherical particles (Fig. 7(a)) and molten HfO_2 that formed a large neck (Fig. 7(b)) were also found from the microstructures of surface.

The cross-sectional SEM images (Fig. 8a) of the tested sample were carefully scrutinized to analyze changes in the aspect of the oxidation layer with respect to the depth from the surface. The dark areas shown at the top, and in the pores of the oxidation layer, are polymer resin that filled in during the mounting process. The oxidation layer was subdivided and magnified into three definite regions from the surface to the matrix (near surface, middle, and near matrix). Considering the images taken in secondary electron mode, the brighter region is composed of heavier elements. Taking into account of the contrast and the EDS analysis obtained from the surface images, the bright granules and the dark phase are HfO_2 and SiO_2 phases, respectively. Based on above results, it is apparent that the bright and fine HfO_2 granules are distributed within SiO_2 in Region 1, which is located near the surface. Some of the SiO_2 phase is also consolidated and cracked in some parts of Region 1. In Region 2, which is located between the surface and the matrix, the SiO_2 phase is mostly located in the upper part (near the surface) and is less evident in the bottom part (near the matrix). Instead, most of the bottom part is HfO_2 with micro-pores. The slightly darker layer in Region 3 is an interlayer located between the matrix layer and delaminated surface layer. The presence of an interlayer is more noticeable in the optical image of the slightly polished surface. When the white surface was removed by polishing, the black-colored interlayer was exposed between the surface oxide and the matrix as shown in Fig. 8b. Based on the EDS results obtained from two different spots (1 and 2) in the BSE image in Fig. 8b, the interlayer consists of Hf, C, and O without Si, although a slight contrast difference is present in the image. The flux of the melted SiO_2 phase from near matrix to outermost layer of the oxidized surface caused the depletion of Si elements from the interlayer. This is similar to the previous study of the oxidation behavior of ZrB_2-SiC composite. The SiC depleted region can be presented in the low pO_2 atmospheric condition due to the evaporation of SiO [34,35]. The evolved SiO gas phase might be evacuated through the melted oxide phases and fully oxidized SiO_2 melted phases were dispersed along HfO_2 grain boundary and filled the crater of surface layer (region 1 from Fig. 8(a)) to form flow/diffusion-blocking barrier. The existence of partially oxidized hafnium phase is similar to the results from previously reported research for the oxidation behavior of HfC ceramic exposed to a CO_2 laser source [36,37].

The oxidation process induced by the oxyacetylene flame is considered to include various thermos-chemical, physical, and mechanical behaviors due to the very high temperature and pressure resulting from the velocity of the combusting gases. Diverse oxidation behaviors at the surface of each sample would be involved during oxyacetylene testing. The reactions possible during the ablation test under the oxyacetylene torch flame are presented below (Eq. (1)–(8)). Although more complex reactions relevant to the presence of oxidants such as H_2O and CO_2 (which would increase the oxidation rate) could also be involved, only the oxidation reactions involving oxygen gas were given for simplicity

Table 1
Comparison of ablation or oxidation properties of UHTC materials.

Materials	Distance between the nozzle and sample(mm)	C_2H_2 flux (l/s)	O_2 flux (l/s)	Max. testing T. (°C)	Max. testing time(s)	Linear reaction thickness(μm)	Linear reaction rate (μm/s)	Ref.
C/C-HfC-SiC	10	0.31	0.42	2580	120	312	2.60	[13]
ZrC coated C/C	10	0.31	0.42	2800	240	62	0.26	[28]
ZrB_2 − 15 vol%SiC	10	0.31	0.42	2400	100	310	3.10	[31]
ZrB_2 − 30vol%SiC	10	0.31	0.42	2400	100	30	0.30	[31]
ZrB_2 − 20vol%SiC	–	0.26	0.53	2200	2400	840	0.35	[18]
HfC − 34vol%SiC	40	0.17	0.22	2800	1800	264	0.14	This study

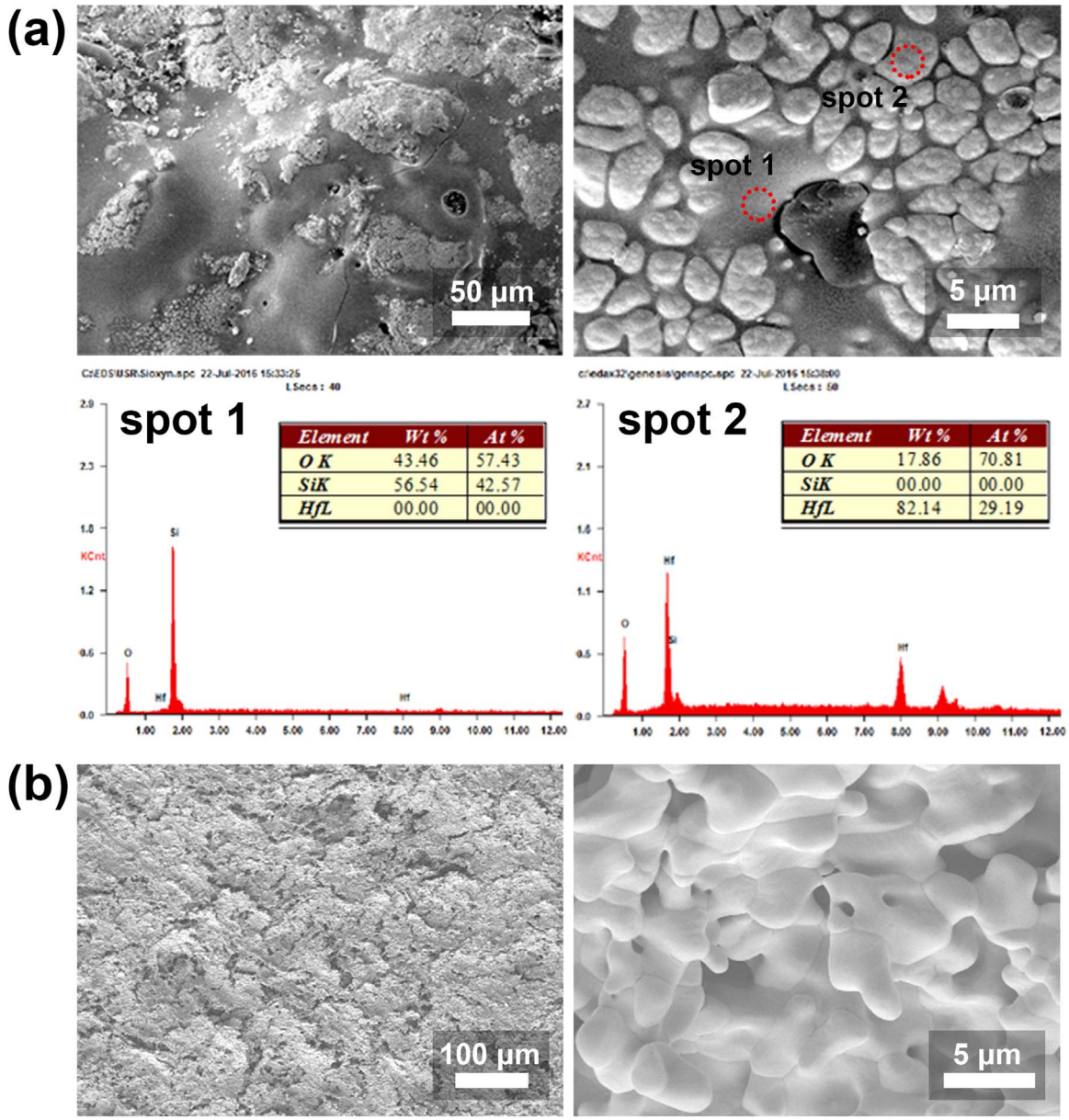

Fig. 7. (a) The surface SEM images after the oxidation test for 20 min and the EDS analysis at the two spots distinguished (spot 1- darkened area, spot 2 - brighter area). (b) The SEM images of the HfO_2 melted phases in the deficient SiO_2 region.

[18].

$$SiC\ (s) + O_2\ (g) \rightarrow SiO_2\ (l) + CO_2\ (g) \quad (1)$$

$$SiC\ (s) + 3/2\ O_2\ (g) \rightarrow SiO_2\ (l) + CO\ (g) \quad (2)$$

$$SiC\ (s) + O_2\ (g) \rightarrow SiO\ (g) + CO\ (g) \quad (3)$$

$$SiO_2\ (l) \rightarrow SiO_2\ (g) \quad (4)$$

$$SiO_2\ (l) \rightarrow SiO\ (g) + 1/2\ O_2\ (g) \quad (5)$$

$$HfC\ (s) + O_2\ (g) \rightarrow HfO_2\ (s) + CO_2\ (g) \quad (6)$$

$$HfC\ (s) + O_2\ (g) \rightarrow HfO_2\ (s) + CO\ (g) \quad (7)$$

$$HfO_2\ (s) \rightarrow HfO_2\ (l) \quad (8)$$

The sequential changes of the HfC-SiC ceramics during the high temperature oxidation test were summarized in Fig. 9 for better understanding of their probable aspects. It is reasonably expected that some of the oxidation reactions above, such as Eqs. 1–3, 6, and 7 occur instantaneously (immediately) when the oxyacetylene torch flame reaches the surface of the samples. These oxidation reactions include the generation of gas phases. The gases are released through the liquid phases at the surface. Considering the boiling point of SiO_2 based on the observed temperature profile, the evaporation of SiO_2 (Eq. (3)) would not have severely occurred during the test. The melted (liquid) SiO_2 phase, which formed near the matrix, flowed both outward and into the pores through the channels between HfO_2 granules by capillary force. This could be seen as evidence that the amount of SiO_2 phase varied with respect to the depth of oxidation from the surface. The oxidation of the HfC-SiC matrix underneath the surface oxidized layer would mainly occur through the instantaneously formed gas evacuation channels in the melted SiO_2 phase. This is because there would be no boundary owing to the presence of melted phases during the oxyacetylene testing. The channels for both evacuation and gas inflow through the oxidation layer would be lengthened by the presence of the HfO_2 granules in the SiO_2 melted phases acting as a flow-blocking barrier. Although the surface oxidation layer is degraded, the combination of melted SiO_2 phase and HfO_2 granules would adhere well to each other, and they

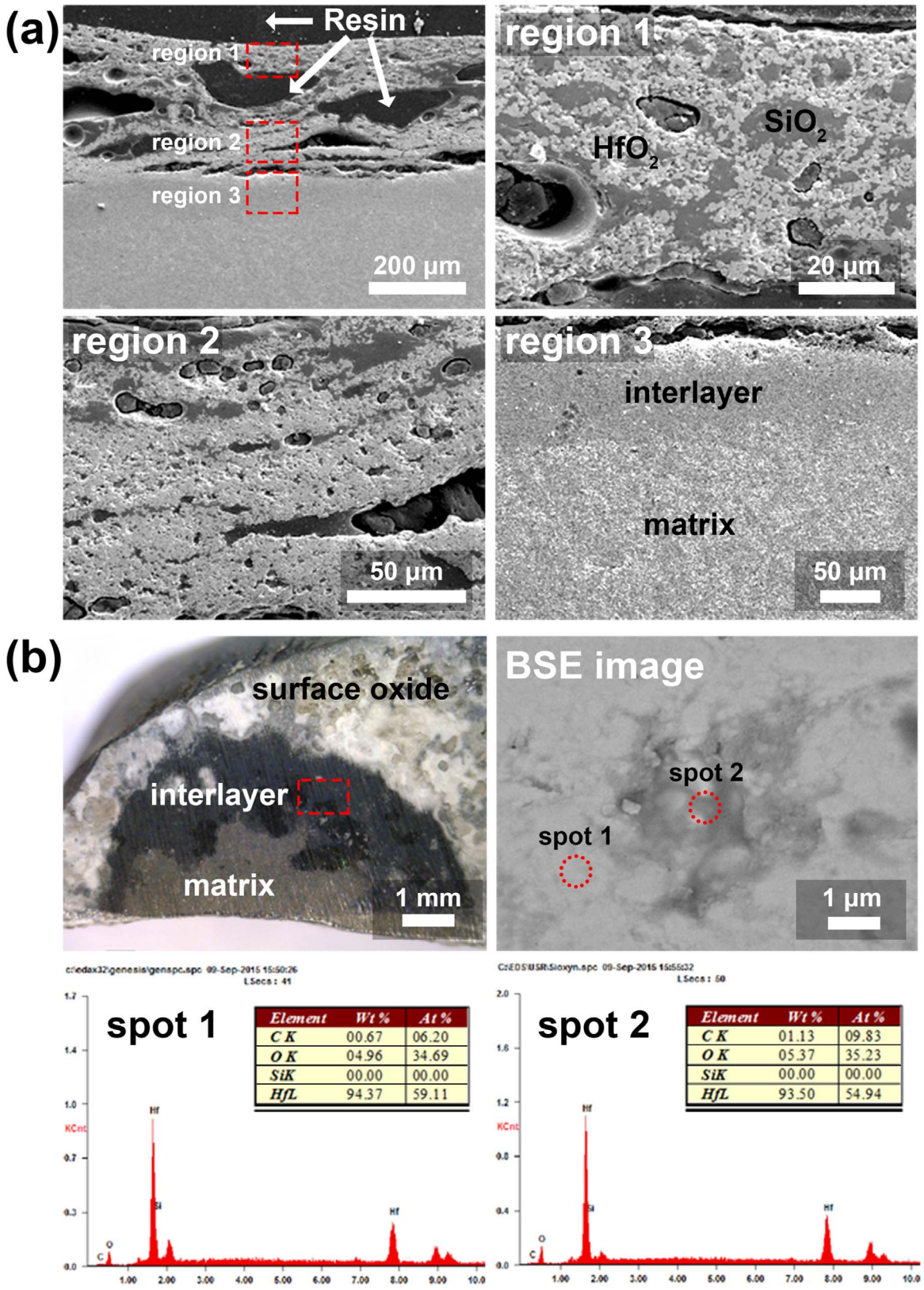

Fig. 8. (a) Magnified cross-sectional SEM images of the HfC-SiC sample tested for 20 min (b) OM image, back-scattered SEM image, and subsequent EDS analysis to confirm the presence of an interlayer between the surface oxidized layer and matrix, and to identify the elements of its composition.

enhance the rigidity of the surface oxidized layer without flowing through the surface or spalling, which could cause severe ablation behaviors. The HfC-SiC composite can persist in spite of such severe test conditions owing to the existence of this well supported surface layer.

4. Conclusions

The high temperature oxidation behaviors of HfC-SiC ceramics prepared via reactive spark plasma sintering were investigated under

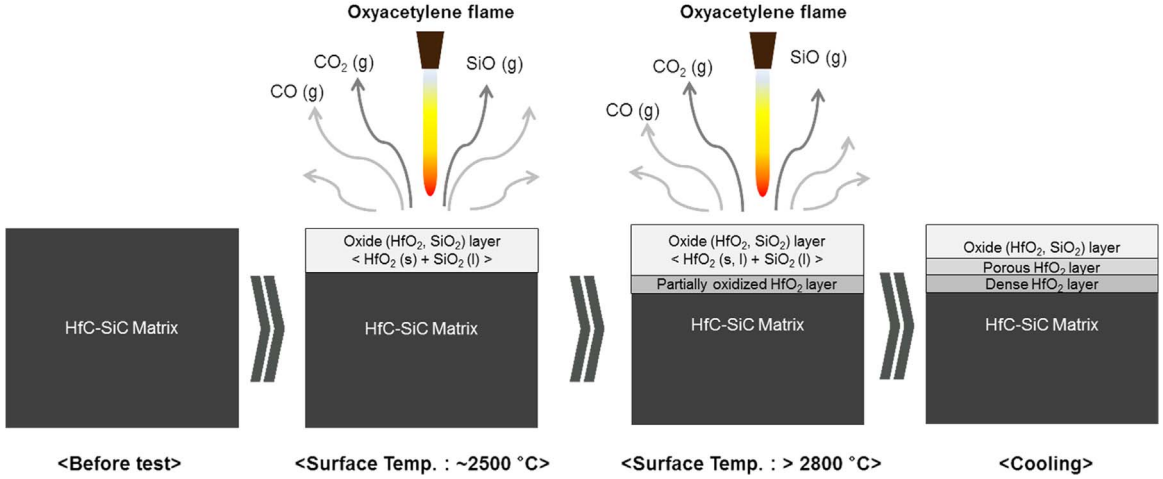

Fig. 9. Schematic illustration of the high-temperature oxidation behaviors of HfC-SiC ceramics under oxyacetylene torch flame.

exposure to the flame of an oxyacetylene torch for up to 30 min. The oxidation rate was determined based on the thicknesses of the oxidized surface layer and the residual matrix. The tested ceramics showed superior resistance to oxidation, compared to previously reported UHTCs materials. The composite structures of the HfO_2 micro-granules and melted SiO_2 phases have crucial roles in the delay of gas flowing from the surface to the interior matrix. An oxygen-deficient hafnium oxide layer was observed near the matrix. The presence of the hafnium oxide layer supports the high temperature oxidation behavior of HfC-SiC ceramics, and follows diffusion-controlled kinetics. This HfC-SiC ceramic is expected to be beneficial as an impregnation material for various kinds of composite matrices such as C-C or C-SiC fiber matrix to improve the ablation and oxidation resistance and to prevent the matrix from the extreme environmental conditions.

Acknowledgements

This work was supported by the R&D Convergence Program of MSIP (Ministry of Science, ICT, and Future Planning) and under framework of the research and development program of the Korea Institute of Energy Research (B8-2416). The authors would like to thank Dr. S. J. Lee in ADD for his valuable comments and theoretical supports.

References

[1] N.P. Bansal, Handbook of ceramic composites, Kluwer Academic Publishers, Boston, 2005.
[2] W. Fahrenholtz, Ultra-high temperature ceramics: materials for extreme environment applications, The America Ceramic Society/Wiley, Hoboken, New Jersey, 2014.
[3] W.G. Fahrenholtz, G.E. Hilmas, I.G. Talmy, J.A. Zaykoski, Refractory diborides of zirconium and hafnium, J. Am. Ceram. Soc. 90 (2007) 1347–1364.
[4] M.M. Opeka, I.G. Talmy, E.J. Wuchina, J.A. Zaykoski, S.J. Causey, Mechanical, thermal, and oxidation properties of refractory hafnium and zirconium compounds, J. Eur. Ceram. Soc. 19 (1999) 2405–2414.
[5] D. Sciti, S. Guicciardi, M. Nygren, Densification and mechanical behavior of HfC and HfB2 fabricated by spark plasma sintering, J. Am. Ceram. Soc. 91 (2008) 1433–1440.
[6] D. Sciti, L. Silvestroni, A. Bellosi, High-density pressureless-sintered HfC-based composites, J. Am. Ceram. Soc. 89 (2006) 2668–2670.
[7] D. Sciti, L. Silvestroni, S. Guicciardi, D.D. Fabbriche, A. Bellosi, Processing, mechanical properties and oxidation behavior of TaC and HfC composites containing 15 vol% TaSi(2) or MoSi(2), J. Mater. Res 24 (2009) 2056–2065.
[8] L. Silvestroni, A. Bellosi, C. Melandri, D. Sciti, J.X. Liu, G.J. Zhang, Microstructure and properties of HfC and TaC-based ceramics obtained by ultrafine powder, J. Eur. Ceram. Soc. 31 (2011) 619–627.
[9] J.X. Liu, X. Huang, G.J. Zhang, Pressureless Sintering of Hafnium Carbide-Silicon Carbide Ceramics, J. Am. Ceram. Soc. 96 (2013) 1751–1756.
[10] L. Feng, S.H. Lee, H.L. Wang, H.S. Lee, Nanostructured HfC-SiC composites prepared by high-energy ball-milling and reactive spark plasma sintering, J. Eur. Ceram. Soc. 36 (2016) 235–238.
[11] Y.H. Seong, S.J. Lee, D.K. Kim, TEM Study of the High-Temperature Oxidation Behavior of Hot-Pressed ZrB2-SiC Composites, J. Am. Ceram. Soc. 96 (2013) 1570–1576.
[12] Y.H. Seong, D.K. Kim, Oxidation behavior of ZrB2-xSiC composites at 1500 degrees C under different oxygen partial pressures, Ceram. Int 40 (2014) 15303–15311.
[13] W.L. Tan, K.Z. Li, H.J. Li, J.P. Zhang, C. Ni, A.Z. Cao, C.H. Ma, Ablation behavior and mechanism of C/C-HfC-SiC composites, Vacuum 116 (2015) 124–129.
[14] Y.J. Wang, H.J. Li, Q.G. Fu, H. Wu, D.J. Yao, H.L. Li, SiC/HfC/SiC ablation resistant coating for carbon/carbon composites, Surf. Coat. Tech. 206 (2012) 3883–3887.
[15] L.Y. Xiang, L.F. Cheng, X.M. Fan, L. Shi, X.W. Yin, L.T. Zhang, Effect of interlayer on the ablation properties of laminated HfC-SiC ceramics under oxyacetylene torch, Corros. Sci. 93 (2015) 172–179.
[16] Y. Yang, K.Z. Li, Z.G. Zhao, H.J. Li, Ablation resistance of HfC-SiC coating prepared by supersonic atmospheric plasma spraying for SiC-coated C/C composites, Ceram. Int. 42 (2016) 4768–4774.
[17] C. Carney, A. Paul, S. Venugopal, T. Parthasarathy, J. Binner, A. Katz, P. Brown, Qualitative analysis of hafnium diboride based ultra high temperature ceramics under oxyacetylene torch testing at temperatures above 2100 degrees C, J. Eur. Ceram. Soc. 34 (2014) 1045–1051.
[18] J.C. Han, P. Hu, X.H. Zhang, S.H. Meng, W.B. Han, Oxidation-resistant ZrB2-SiC composites at 2200 degrees C, Compos. Sci. Technol. 68 (2008) 799–806.
[19] L.M. Huang, Y. Xiang, F. Cao, R.J. Liu, C.R. Zhang, The degradation behavior of UHTCs based coatings coated PIP-C/SiC composites in thermal cycling environment, Compos. Part B-Eng. 86 (2016) 126–134.
[20] C.Y. Li, K.Z. Li, H.B. Ouyang, J.F. Huang, H.J. Li, Y.L. Zhang, J. Fei, X.G. Kong, Effect of ZrO2 morphology on the ablation resistance of carbon/carbon composites containing ZrC prepared by the carbothermal reduction reaction, Corros. Sci. 102 (2016) 405–412.
[21] W. Li, Y. Xiang, S. Wang, Y. Ma, Z.H. Chen, Ablation behavior of three-dimensional braided C/SiC composites by oxyacetylene torch under different environments, Ceram. Int 39 (2013) 463–468.
[22] Y.Y. Li, Q.G. Li, Z. Wang, L.L. Lv, Oxidation behavior of laminated ZrB2-SiC composites and monolithic ZrB2-SiC composites, Ceram. Int 42 (2016) 2063–2069.
[23] C.H. Ma, L.J. Guo, H.J. Li, W.L. Tan, T. Duan, N.K. Liu, M.Y. Zhang, Effects of high-temperature annealing on the microstructures and mechanical properties of C/C-ZrC-SiC composites prepared by precursor infiltration and pyrolysis, Mater. Des. 90 (2016) 373–378.
[24] M. Miller-Oana, P. Neff, M. Valdez, A. Powell, M. Packard, L.S. Walker, E.L. Corral, Oxidation Behavior of Aerospace Materials in High Enthalpy Flows Using an Oxyacetylene Torch Facility, J. Am. Ceram. Soc. 98 (2015) 1300–1307.
[25] A. Paul, J.G.P. Binner, B. Vaidhyanathan, A.C.J. Heaton, P.M. Brown, Heat flux mapping of oxyacetylene flames and their use to characterise Cf-HfB2 composites, Adv. Appl. Ceram. 115 (2016) 158–165.
[26] A. Paul, S. Venugopal, J.G.P. Binner, B. Vaidhyanathan, A.C.J. Heaton, P.M. Brown, UHTC-carbon fibre composites: preparation, oxyacetylene torch testing and characterisation, J. Eur. Ceram. Soc. 33 (2013) 423–432.
[27] W.N. Tan, M. Adducci, R. Trice, Evaluation of rare-earth modified ZrB2-SiC ablation resistance using an oxyacetylene torch, J. Am. Ceram. Soc. 97 (2014) 2639–2645.
[28] S.L. Wang, K.Z. Li, H.J. Li, Y.L. Zhang, T. Feng, Structure evolution and ablation behavior of ZrC coating on C/C composites under single and cyclic oxyacetylene torch environment, Ceram. Int 40 (2014) 16003–16014.
[29] Y.L. Wang, X. Xiong, G.D. Li, H.B. Zhang, Z.K. Chen, W. Sun, X.J. Zhao, Microstructure and ablation behavior of hafnium carbide coating for carbon/carbon composites, Surf. Coat. Tech. 206 (2012) 2825–2832.
[30] W. Yong-Jie, L. He-Jun, F. Qian-Gang, W. Heng, Y. Dong-Jia, W. Bing-Bo, Ablative property of HfC-based multilayer coating for C/C composites under oxy-acetylene torch, Appl. Surf. Sci. 257 (2011) 4760–4763.
[31] X. Zhang, Z.K. Chen, X. Xiong, R.T. Liu, Y.Y. Zhu, Morphology and microstructure of ZrB2-SiC ceramics after ablation at 3000 degrees C by oxy-acetylene torch, Ceram. Int 42 (2016) 2798–2805.
[32] L. Zhuang, Q.G. Fu, B.Y. Tan, Y.A. Guo, Q.W. Ren, H.J. Li, B. Li, J.P. Zhang, Ablation

behaviour of C/C and C/C-ZrC-SiC composites with cone-shaped holes under an oxyacetylene flame, Corros. Sci. 102 (2016) 84–92.
[33] J.-H. Kim, C.Y. Baek, D.S. Kim, S.T. Lim, D.K. Kim, Interfacial microstructure of diffusion-bonded W-25Re/Ti/graphite joint and its high-temperature stability, Korean J. Mater. Res. 26 (2016) 751–756.
[34] W.G. Farenholtz, Thermodynamic analysis of ZrB2-SiC oxidation: formation of a SiC-Depleted Region, J. Am. Ceram. Soc. 90 (2007) 143–148.
[35] A. Rezaie, W.G. Farenholtz, G.E. Hilmas, Evolution of structure during the oxidation of zirconium diboride-silicon carbide in air up to 1500 °C, J. Eur. Ceram. Soc. 27 (2007) 2495–2501.
[36] C.B. Bargeron, R.C. Benson, X-ray-microanalysis of a hafnium carbide film oxidized at high-temperature, Surf. Coat. Tech. 36 (1988) 111–115.
[37] C.B. Bargeron, R.C. Benson, A.N. Jette, T.E. Phillips, Oxidation of hafnium carbide in the temperature-range 1400° to 2060 °C, J. Am. Ceram. Soc. 76 (1993) 1040–1046.